
IVUS image processing and semantic analysis for Cardiovascular Diseases risk prediction

**Charalampos Doulaverakis*,
Maria Papadogiorgaki, Vasileios Mezaris,
Antonis Mpilllis, Eirini Parissi
and Ioannis Kompatsiaris**

Informatics and Telematics Institute,
Center for Research and Technology Hellas,
1st km, Thermi-Panorama Road, Thessaloniki 57001, Greece

E-mail: doulaver@iti.gr E-mail: mpapad@iti.gr

E-mail: bmezaris@iti.gr E-mail: antonis@iti.gr

E-mail: parissi@iti.gr E-mail: ikom@iti.gr

*Corresponding author

Anastasios Gounaris

Department of Informatics,
Aristotle University of Thessaloniki,
541 24 Thessaloniki, Greece
E-mail: gounaria@csd.auth.gr

**Yiannis S. Chatzizisis
and George D. Giannoglou**

Cardiovascular Engineering and Atherosclerosis Laboratory,
1st Cardiology Department,
AHEPA University Hospital,
School of Medicine, Aristotle University of Thessaloniki,
1st Kyriakidi Str, GR54636 Thessaloniki, Greece
E-mail: joc@med.auth.gr
E-mail: yan@med.auth.gr

Abstract: The work presented in this paper is part of a system able to perform risk classification of patients based on medical image analysis and on the semantically structured information of patient data from medical records and biochemical data. More specifically, the paper focuses on Intravascular Ultrasound (IVUS) image processing and the automated segmentation developed to extract the useful arterial boundaries. This is coupled with the design and implementation of a semantic reasoning-enabled knowledge base in OWL that integrates data from heterogeneous sources and incorporates functionality for DL classification. Performance evaluation of both IVUS image processing and knowledge base is discussed.

Keywords: IVUS image processing; RBF; radial basis function; risk prediction; semantic analysis; OWL; SWRL.

Reference to this paper should be made as follows: Doulaverakis, C., Papadogiorgaki, M., Mezaris, V., Mpillis, A., Parissi, E., Kompatsiaris, I., Gounaris, A., Chatzizisis, Y.S. and Giannoglou, G.D. (xxxx) 'IVUS image processing and semantic analysis for Cardiovascular Diseases risk prediction', *Int. J. Biomedical Engineering and Technology*, Vol. x, No. x, pp.xxx-xxx.

Biographical notes: Charalampos Doulaverakis received his Diploma in Electronic and Computer Engineering from the Technical University of Crete, Greece, in 2003 and his MSc in Advanced Computing from the Aristotle University of Thessaloniki, Greece, in 2008. Since 2004, he is a Research Associate with the Informatics and Telematics Institute/Center for Research and Technology Hellas, Thessaloniki, Greece. His research interests include image processing, ontology engineering and semantic web. He is a Member of the Technical Chamber of Greece.

Maria Papadogiorgaki received the Diploma in Electrical and Computer Engineering and the MSc in Medical Informatics from the Aristotle University of Thessaloniki, Thessaloniki, Greece, in 2003, and 2006, respectively. Since 2003, she is a Research Assistant with the Informatics and Telematics Institute/Center for Research and Technology Hellas, Thessaloniki, Greece. Her research interests include medical image analysis/processing, machine learning and personalisation systems. She is a Member of the Technical Chamber of Greece.

Vasileios Mezaris received the Diploma and the PhD in Electrical and Computer Engineering from the Aristotle University of Thessaloniki, Thessaloniki, Greece, in 2001 and 2005, respectively. He is a Senior Researcher (Researcher D) with the Informatics and Telematics Institute/Center for Research and Technology Hellas, Thessaloniki, Greece. His research interests include image and video analysis, content-based and semantic image and video retrieval, ontologies, multimedia standards, knowledge-assisted multimedia analysis, knowledge extraction from multimedia, medical image analysis. He is a member of the IEEE and the Technical Chamber of Greece.

Antonis Mpillis received the Diploma in Electrical and Computer Engineering from the Aristotle University of Thessaloniki, Thessaloniki, Greece, in 2007 where he is currently attending the graduate programme of Medical Informatics, co-organised by the Medical School, the Engineering Faculty and the Faculty of Sciences. He is also a Graduate Research Assistant with the Informatics and Telematics Institute, Thessaloniki, Greece. His research interests include biomedical engineering, image and video processing and networking protocols. He is a Member of the Technical Chamber of Greece.

Eirini Parissi graduated from the Electrical Engineering Department of Aristotle University of Thessaloniki in 2005 and worked as a Research Assistant in the Multimedia Knowledge Lab, Informatics and Telematics Institute, CERTH/ITI, until December 2007. Her basic regions of interest have been medical image processing, ontology engineering and reasoning support, focusing onto medical applications. She is currently in the second year of studies of Master in Business Administration in the University of Macedonia, Thessaloniki, Greece.

Ioannis Kompatsiaris received the Diploma in Electrical Engineering and the PhD in 3-D Model based Image Sequence Coding from Aristotle University of Thessaloniki, Greece, in 1996 and 2001, respectively. He is a Senior Researcher (Researcher B') with the Informatics and Telematics Institute. His research interests include semantic multimedia analysis, indexing and retrieval, multimedia and the semantic web, knowledge structures, reasoning and personalisation for multimedia applications. He is the co-author of ten book chapters, 30 papers in refereed journals and more than 90 papers in international conferences. He is a Member of IEEE, ACM and IEE.

Anastasios Gounaris is a Lecturer at the Department of Informatics of the Aristotle University of Thessaloniki, Greece. Prior to that, he was a Visiting Lecturer with the University of Cyprus, a Research Associate with the School of Computer Science of the University of Manchester and he has also collaborated with the ITI Institute of the Center of Research and Technology – Hellas CERTH. He received his PhD from the University of Manchester (UK) in 2005. He is a Member of the Technical Chamber of Greece, ACM, and IEEE. This work was conducted while he was with ITI-CERTH

Yiannis S. Chatzizisis received the MD from the Medical School, Aristotle University of Thessaloniki (A.U.Th), Thessaloniki, Greece, in 2000, and the MSc from the same university in 2004. Since 2004, he is a PhD candidate in A.U.Th. with funding from the Greek State Scholarships Foundation. In 2005, he completed the Residency in Internal Medicine at the AHEPA University Hospital, Thessaloniki, Greece. Since 2000, he has been a Research Fellow in Cardiology at the Cardiovascular Engineering and Atherosclerosis Laboratory, A.U.Th. Since 2005, he has been Research Fellow in Cardiology at the Brigham and Women's Hospital, Harvard Medical School and the Massachusetts Institute of Technology. He is now Cardiology Fellow at the AHEPA University Hospital, Thessaloniki, Greece. His research interests include molecular biology of atherosclerosis, cardiovascular fluid dynamics, and cardiovascular imaging.

George Giannoglou graduated from Medical School of Aristotle University of Thessaloniki in 1971. He is Professor of Cardiology at the 1st Cardiology Department, AHEPA University General Hospital, Thessaloniki, Greece. His research interests include the study of pathophysiology of atherosclerosis with special focus on the effect of local haemodynamic factors (e.g., shear stress, wall stress). Furthermore, he is working on the development of Intravascular Ultrasound (IVUS)-based methods for the imaging of atherosclerotic lesions.

1 Introduction

Today, the delivery of healthcare services to patients relies heavily on Medical Information Systems. Such systems are based on cutting-edge information technology to electronically collect, process, examine, distribute, display and store patient data. The increasing volume of medical data demands new techniques for organising, sharing, managing and extracting knowledge. The extracted knowledge can then be used to facilitate disease diagnosis, prevent human error and inform about the functions and consequences of several diseases. Ontologies and Semantic Web technologies can offer solutions to medical information management problems, such as the navigation

and integration of large and complex medical terminologies (Nelson et al., 2002). These efforts have resulted in thesauri and meta-thesauri like the MeSH and UMLS. They are mainly used for medical document classification and retrieval purposes, but other major uses include term disambiguation and medical systems interoperability, which can in turn offer decision-support and knowledge reuse in areas such as breast cancer diagnosis from X-ray mammography and MRI images, and coronary artery disease prognosis.

Additionally, advances in digital signal processing and, more specifically, image analysis, take a major hand in medical progress, as analysis of medical images plays an ever-increasing crucial role in terms of medical diagnosis and research. In the field of medical imaging, coronary angiography is acknowledged as the gold standard for imaging and diagnosis of coronary heart disease (Nissen and Yock, 2001). However, it is restricted by its inability to depict the vessel wall, provided that it illustrates the coronary arteries as a silhouette of the lumen. Thus, it fails to quantify plaque burden, which is responsible for partial or total obstruction of the arteries. Recently, Intravascular Ultrasound (IVUS) has been introduced as complementary to angiography diagnostic technique aiming at more accurate imaging of coronary atherosclerosis (Bom et al., 1998; Mario et al., 1998). The detection of specific features in IVUS images constitutes a necessary step for accurate morphometric analysis of coronary plaques and accordingly the assessment of the atherosclerotic lesion length (Schoenhagen and Nissen, 2002).

One of the medical research areas that can benefit from advances in the above-mentioned technologies is that of Cardiovascular Diseases (CVDs). CVDs, but principally heart disease and atherosclerosis, are worldwide primarily fatal diseases for both men and women among all racial and ethnic groups. According to data from the American Heart Association, almost 1 million Americans die of CVD each year, which adds up to 42% of all deaths. Atherosclerosis involves a build-up on the inner side of artery walls. Excess fat or plaque deposits are narrowing the veins that supply oxygenated blood to the heart, usually leading to a heart attack. There is overwhelming evidence that high blood cholesterol increases the risk of developing atherosclerosis (Glagov et al., 1987).

Following the above studies, the work presented in this paper is part of a bioinformatics system utilising real 3D reconstruction of coronary arteries, by fusion of IVUS and biplane angiography imaging, along with Computational Fluid Dynamics (CFD) techniques to provide early diagnosis of coronary arteries diseases. The system is also able to perform risk classification of patients based on the semantically structured information of patient data. The paper focuses on two major parts of the system, i.e., the IVUS image processing and segmentation module and on the design and implementation of the semantic reasoning-enabled knowledge base in Web Ontology Language (OWL) that integrates data from heterogeneous sources, such as images and structured files, and incorporates functionality for Description Logic (DL) classification.

More specifically, regarding IVUS image segmentation, the paper presents an automated method for the segmentation of IVUS images and specifically for the detection of luminal and medial–adventitial boundaries, based on the results of texture analysis, performed by means of a multilevel Discrete Wavelet Frames (DWFs) decomposition, and on a smoothing step using Radial Basis Function (RBF) approximation. The proposed approach does not require manual initialisation of the

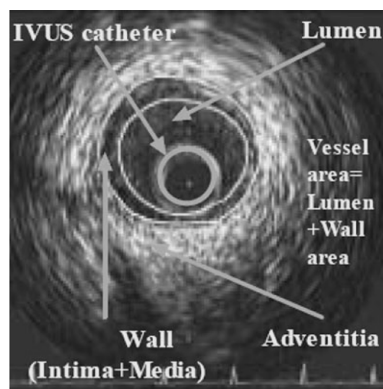
contours and shows promising results. Regarding the semantic data processing, research focuses on risk prediction of CVDs, employing Semantic Web to achieve interoperability, clarity, unambiguity and proof tracing. All patient data, including those coming from automated IVUS image analysis, are expressed as classes and properties of an OWL medical ontology using standard terminology adopted from the MeSH thesaurus.

The remainder of the paper is structured as follows: Section 2 gives a detailed description of the proposed methodology for IVUS image processing, while Section 3 elaborates on the employed knowledge-based risk assessment system by giving insights in the ontology and rules used as foundations of the knowledge base. Results on the IVUS segmentation method and evaluation of knowledge base performance and scalability are discussed in Section 4. Section 5 concludes the paper with a discussion about plans for future work.

2 IVUS image processing

IVUS is a catheter-based technique that renders two-dimensional images of coronary arteries and, therefore, provides information concerning luminal and wall area, plaque morphology and wall composition (Figure 1). The wall of coronary arteries consists of three main layers: intima, media and adventitia, while three regions are visualised as distinguished fields in an IVUS image, namely the lumen, the vessel wall (consisted of the intima and the media layers) and the adventitia plus surroundings, as illustrated in Figure 1. The above-mentioned regions are separated by two closed contours: the inner border, which corresponds to the lumen–wall interface, and the outer border representing the boundary between media and adventitia. The reliable and quick detection of these two borders is the goal of analysis and also the basic step towards the subsequent 3D reconstruction of the arteries, which can provide additional information regarding the burden of atherosclerosis (Giannoglou et al., 2006). However, the quantitative evaluation of characteristic parameters such as luminal and wall area that is necessary for the clinical evaluation of the image data requires their segmentation according to the actual structure of the coronary arteries.

Figure 1 IVUS image



2.1 *Related work*

A direct approach to IVUS image analysis is manual segmentation, i.e., the manual determination of the inner and outer borders, which is always performed by an expert. It is a time-consuming procedure with results affected by the high inter- and intra-user's variability. To overcome these limitations, several approaches for semi-automated segmentation have been proposed in the literature. Semi-automated methods include a usually crude and fast manual denotation of the vessel borders followed by an automated refinement to depict as precisely as possible the actual borders. Sonka et al. (1995) implemented a knowledge-based graph searching method incorporating a priori knowledge on coronary artery anatomy and a selected region of interest prior to the automatic border detection. Quite a few variations of the active contour model have been investigated. The active contour principles have been used to allow the extraction of the borders in three dimensions after setting an initial contour in Kovalski et al.'s (2000) approach. However, the contour detection fails for low-contrast interface regions such as the luminal border where the blood-wall interface in most images corresponds to weak pixel intensity variation. Klingensmith et al. (2004) employ plaque characterisation by using the frequency information to improve the active surface segmentation algorithms after acquiring the Radiofrequency (RF) IVUS data.

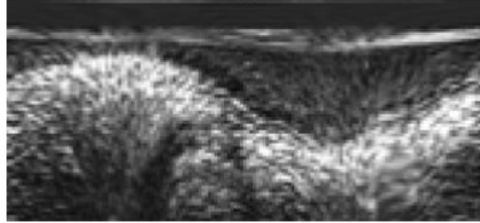
For clinical practice, the most attractive approaches are the fully automatic ones with a limited number of them being developed so far. Brusseau et al. (2004) exploited an automatic method for detecting the endoluminal border based on an active contour that evolves until it optimally separates regions with different statistical properties. Giannoglou et al. (2007) propose an automated segmentation method based on a variant of the active contour model, while Filho et al. (2005) investigated a fuzzy clustering algorithm for adaptive segmentation in IVUS images. Cardinal et al. (2006) present a 3D IVUS segmentation where Rayleigh probability density functions are applied for modelling the pixel grey value distribution of the vessel wall structures. An automated approach based on deformable models has been reported by Plissiti et al. (2004), who employed a Hopfield neural network for the modification and minimisation of an energy function as well as a priori vessel geometry knowledge. Unal et al. (2006) proposed a shape-driven approach to the segmentation of IVUS images, based on building a shape space using training data and consequently constraining the lumen and media-adventitia contours to a smooth, closed geometry in this space.

2.2 *Image pre-processing*

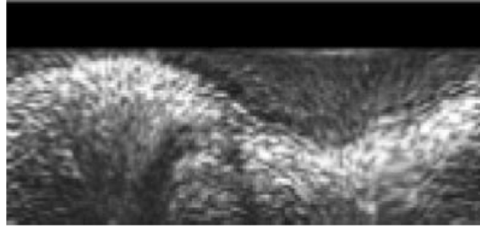
The proposed method, described in detail in Papadogiorgaki et al. (2007a, 2007b), involves a pre-processing of the image data for the purpose of applying texture description. The method consists of two steps: representation of the images in polar coordinates (Figure 2(a)), and removal of catheter-induced artefacts (Figure 2(b)). Representation of the images in polar coordinates is important for facilitating the description of local image regions in terms of their radial and tangential characteristics. Each of the original IVUS images is transformed to a polar coordinate image where columns and rows correspond to angle and distance from the centre of the catheter, respectively, and this image alone, denoted $I(r, \theta)$, is used throughout the analysis process.

The images produced by IVUS include not only tissue and blood regions but also the outer boundary of the catheter itself. The latter defines a dead zone of radius equal to that of the catheter, where no useful information is contained. Knowing the diameter of the catheter, these catheter-induced artefacts are easily removed by setting $I(r, \theta) = 0$ for $r < D/2 + e$, e being a small constant. This pre-processing is illustrated in Figure 2.

Figure 2 (a) IVUS image in polar coordinates and (b) IVUS image after catheter removal



(a)



(b)

2.3 Contour initialisation

Prior to contour initialisation, texture analysis is employed, as it has been proven to be an important cue for image analysis (Mezaris et al., 2004). DWFs (Unser, 1995) have been used for texture analysis, a method similar to Discrete Wave Transform (DWT) that uses a filter bank to decompose the greyscale image to a set of sub-bands. The filter bank is based on the low-pass Haar filter $H(z) = (1/2)(1 + z^{-1})$ and its complementary high-pass filter $G(z) = zH(-z^{-1})$. A four-level DWF is employed using the fast iterative Texture Analysis and RBF approximation proposed by Unser (1995), resulting in $K = 12$ images where each image, denoted as I_k , $k = 1, \dots, K$, results from treating each calculated standard deviation from the neighbourhood F of pixel p as intensity value for pixel p . In addition to these images, an approximation component that is a low-pass filtered image denoted as I_{LL} is generated.

Following the texture analysis, the objective of the contour initialisation procedure is the detection of pixels that are more likely to belong to the lumen and media–adventitia boundaries. On the basis of the proposed approach, the initialisation of the lumen boundary relies on the observation that the lumen and wall areas demonstrate different texture characteristics: the lumen area tends to be a low-intensity non-textured region, with noise being responsible for any high-intensity artefacts in it, whereas the wall area is typically characterised by the presence of both low-intensity and high-intensity parts, with changes between the two are of relatively low-frequency in the tangential direction

and of somewhat higher frequency in the radial direction. Consequently, the local energy of the signal in appropriate frequency sub-bands can be used as a criterion for differentiating between the lumen and wall areas; to this end, the results of texture analysis discussed in the previous paragraph are employed.

Regarding the initialisation of the media–adventitia boundary, the approximation component of the DWF decomposition is used. This choice was motivated by the observation that in many cases the media–adventitia boundary is represented by a thick bright ring (a thick bright curve in polar coordinates) that is dominant in the IVUS image. Thus, in the approximation component, the media–adventitia boundary is rather well preserved, as opposed to higher-frequency details that are suppressed by the low-pass filtering, which facilitates contour initialisation.

In detail, let $I_{\text{int}}, I_{\text{ext}}$ denote the simplified images, after texture analysis, which are used for detecting the lumen and media–adventitia boundaries, respectively. These are defined based on the proposed approach as

$$I_{\text{int}}(r, \theta) = \frac{255}{\max_{r, \theta} \{I'_{\text{int}}(r, \theta)\}} \{I'_{\text{int}}(r, \theta)\} \quad (1)$$

$$I'_{\text{int}}(r, \theta) = \sum_k I_k(r, \theta) \quad (2)$$

$$I_{\text{ext}}(r, \theta) = I_{LL}(r, \theta). \quad (3)$$

The choice of images I_k that are employed in this initialisation process was done based on visual evaluation of all K generated images and is in line with the aforementioned observations regarding the texture properties of the lumen and wall areas, in combination with the characteristics of the filter bank used for the generation of images I_k .

The internal contour is initialised as the set of pixels

$$c_{\text{int}} = \{p_{\text{int}} = [\rho, \theta]\} \quad (4)$$

for which

$$I_{\text{int}}(\rho, \theta) > T \text{ and } I_{\text{int}}(r, \theta) < T, \quad \forall r < \rho \quad (5)$$

thus defining an internal contour function $c_{\text{int}}(\theta) = \rho$ (Figure 3(a)) T in the above equation is a threshold whose value was set experimentally to 128; small deviations from this value were shown to have little effect on the results of initialisation.

The external contour is initialised as the set of pixels:

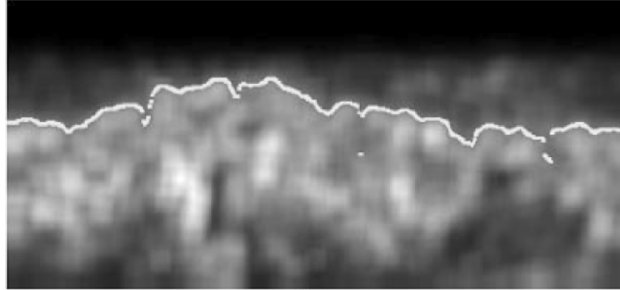
$$c_{\text{ext}} = \{p_{\text{ext}} = [\mu, \theta]\} \quad (6)$$

for which

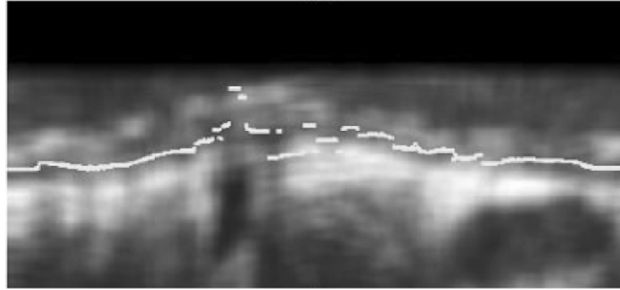
$$I_{\text{ext}}(\mu, \theta) = \max_{r > \rho} \{I_{\text{ext}}(r, \theta)\} \quad (7)$$

where $[\rho', \theta]$ are the points of the final internal contour, as obtained by applying to the initialisation data the refinement process of the following section. This defines a contour function $c_{\text{ext}}(\theta) = \mu$ for the external contour (Figure 3(b)).

Figure 3 Results of contour initialisation for: (a) the lumen and (b) the media–adventitia boundary



(a)



(b)

2.4 Contour refinement using Radial Basis Function approximation

In contrast to the initial contours generated as described in the previous paragraph, which are not smooth and are characterised by discontinuities (Figure 3, the true lumen and media–adventitia boundaries are smooth, continuous functions of θ). Consequently, to obtain smooth contours that are consistent with the true ones, the application of a filtering or approximation procedure to the initial contour functions $c_{\text{int}}(\theta)$, $c_{\text{ext}}(\theta)$ is required. In this work, RBFs (Carr et al., 2001) are used for this purpose.

Polyharmonic RBFs have been proposed for reconstructing smooth, manifold surfaces from point-cloud data and for repairing incomplete meshes through interpolation methods and approximation techniques. Their suitability for contour refinement in the IVUS image segmentation process has been investigated by Papadogiorgaki et al. (2007a, 2007b). Using them for the approximation of the initial contours in a frame, i.e., the generation of a contour c' that is a smooth, reasonable approximation of c requires the definition for each such contour of a function f as follows:

$$f(\theta, C(\theta)) = 0 \quad (8)$$

where $C(\theta)$ here denotes either $c_{\text{int}}(\theta)$ or $c_{\text{ext}}(\theta)$, depending on the contour being examined. Function f is used for formulating the approximation problem as the one of finding an RBF s for which $s(\cdot) \cong f(\cdot)$. To avoid the trivial solution of s being zero at

every point, f must also be defined for a set of points not belonging to the initial contour, so that

$$f(\theta, r \neq C(\theta)) \neq 0. \quad (9)$$

The latter points are defined in this work as those that satisfy the following equations:

$$r = \max_{\theta} C(\theta) + 1 \quad (10)$$

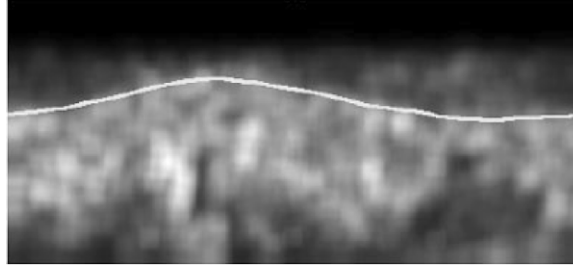
$$r = \max_{\theta} C(\theta) - 1. \quad (11)$$

For the above points in the 2D space, function f is defined as the signed Euclidean distance from the initialised contour for $\theta = \text{const}$, i.e.,

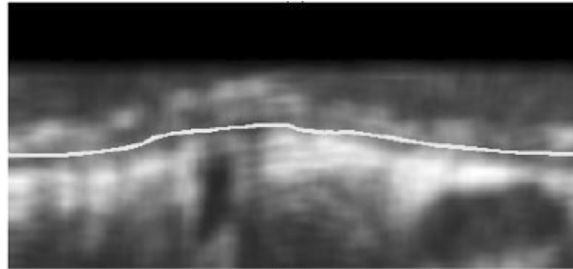
$$f(\theta, r \neq C(\theta)) \neq r - C(\theta). \quad (12)$$

Following the definition of f , the FastRBF library (FarField Technology) was used to generate the smooth contour approximation c' by removing duplicate points where f has been defined (i.e., points in the 2D space which are located within a specific minimum distance from other input points), fitting of an RBF to this data and evaluating it to find the points, which correspond to zero value; the latter defines the contour approximation c' . Figure 4 shows the result of applying the RBF-based refinement on the contours of Figure 3.

Figure 4 (a, b) The result of the proposed contour refinement method applied to the contours of Figure 3(a) and (b) respectively



(a)



(b)

After the successful detection of the inner and outer borders, morphometric analysis for the estimation of important vessel parameters takes place. Using the detected borders as reference, the centre of mass for the lumen is calculated and we proceed to the measurement of the dimensions as depicted in Figure 5. Point A is the centre of mass while AB is defined as the lumen radius and BC is the Wall Thickness. The sum of AB and BC is the vessel radius. Owing to the shape of the vessel, almost every dimension measurement that is calculated will be different from each other, so a number of measurements have to be taken. Typically, 200 radii and Wall Thickness measurements are calculated for every IVUS image so as to estimate the mean vessel and lumen radius. The largest and the smallest Wall Thickness values, denoted as $maxWT$ and $minWT$ in Figure 5, are also registered, as they provide important clues to the development of atheromatic plaque on the artery. Additionally, the area of the lumen, wall and vessel is calculated. Table 1 summarises the parameters measured from every IVUS image.

Figure 5 Calculated artery measurements for morphometric analysis. WT represents Wall Thickness

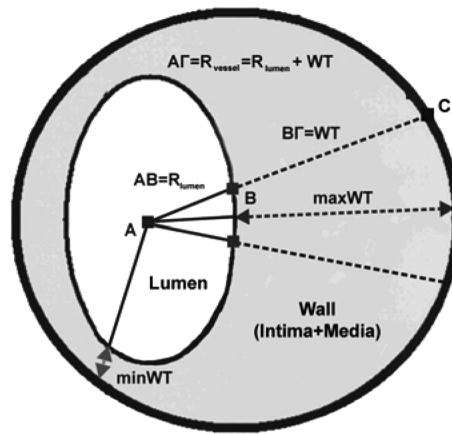


Table 1 Parameters calculated for every IVUS image

<i>Parameter</i>	<i>Symbol</i>	<i>Units</i>
Vessel area	E_{vessel}	mm^2
Lumen area	E_{lumen}	mm^2
Wall area	E_{wall}	mm^2
Vessel min radius	$minR_{vessel}$	mm
Vessel max radius	$maxR_{vessel}$	mm
Vessel mean radius	$meanR_{vessel}$	mm
Lumen min radius	$minR_{lumen}$	mm
Lumen max radius	$maxR_{lumen}$	mm
Lumen mean radius	$meanR_{lumen}$	mm
Vessel min diameter	$minD_{vessel}$	mm
Vessel max diameter	$maxD_{vessel}$	mm
Vessel mean diameter	$meanD_{vessel}$	mm

Table 1 Parameters calculated for every IVUS image (continued)

<i>Parameter</i>	<i>Symbol</i>	<i>Units</i>
Lumen min diameter	$\text{minD}_{\text{lumen}}$	mm
Lumen max diameter	$\text{maxD}_{\text{lumen}}$	mm
Lumen mean diameter	$\text{meanD}_{\text{lumen}}$	mm
Mean Wall Thickness	meanWT	mm
Max Wall Thickness	maxWT	mm
Min Wall Thickness	minWT	mm

3 Semantic medical data processing

Semantic analysis and classification are applied to facilitate the examination of IVUS image sequences and extract initial knowledge-based diagnosis of coronary artery disease. The preliminary diagnosis is achieved through an end-to-end analysis of raw medical facts via the image processing procedure described earlier, in combination with complex reasoning tasks. At a first level, the developed medical ontology provides a central point for accumulation of information produced from different modalities, i.e., analysis of IVUS images, data collected from patient's medical record and from biochemical tests, where they are automatically arranged and stored in a structured ontological form. At a second level of process, semantic rules and inherent reasoning capabilities of ontologies are applied to the data to perform the required classification. Using this approach, a core knowledge base of patients is created.

Benefits from this procedure are easy to conceive. One of the most important aspects is that data would be otherwise distributed among different sections or databases of a hospital, e.g., IVUS images would remain in the Cardiovascular Laboratory separated from biochemical and medical record data thus complicating or making difficult the amassment and processing of the data. Another key benefit comes from the ontology itself as it allows the semantic and, in turn, automatic further processing of information. Semantic description of data or information in the area of medicine has proven to be quite useful.

The medical domain offers a rich and often non-monotonically defined vocabulary. An example, taken from the MeSH thesaurus, is the term *Diabetes Mellitus*, which can have the meaning either of a *Metabolic Disorder* or of an *Endocrine System Disease*. Through the ongoing research (MeSH, UMLS), there is an effort to organise all medical terms and concepts in a semantic structure so as to avoid ambiguity of term meanings (Nelson et al., 1999). Making use of such outcomes has the advantage of dramatically decreasing the development time to conceptualise the medical domain of interest in a given application as is the case with the presented system.

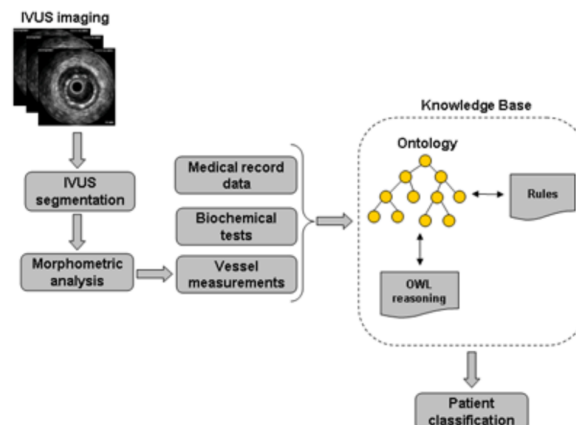
With the ongoing progress that is being constantly made in the area of knowledge management through ontologies, medical information systems are shifting to the use of standardised terminologies and hierarchies. Such standardisation actions are, as already mentioned, the Medical Subject Headline (MeSH), which is a thesaurus used primarily for the indexing of medical documents, the Unified Medical Language System (UMLS), which provides a semantic network of concepts aiming at the development of advanced information systems, and the OpenGALEN Ontology of Human Anatomy project aiming

at providing semantic hierarchy of clinical guidelines to be followed by healthcare personnel (Rogers et al., 2001). The incorporation of widely accepted ontologies or thesauri in the development of medical information will enable the interoperation of these systems even at an international level, as the main effort in these actions is to formalise knowledge at a semantic rather than a linguistic level, thus paving the way to unified or interoperable medical information systems.

The work presented in this paper makes use of such outcomes. In the development of our domain ontology, the MeSH thesaurus was used as a reference. Following specific guidelines, given by the medical experts in the project, on the data to be integrated and on the needed classification and assumptions in the semantic analysis system, the appropriate concepts from the thesaurus were selected and, by retaining hierarchy, gathered to create the OWL ontology. Use of the latter to create the core knowledge base can ensure future scaling of the system to support interoperability as previously described.

The semantic analysis and classification approach layout is presented in Figure 6. The main idea is based on linking measurements extracted from IVUS images, as well as patient record information and biochemical data, to a conventional Semantic Web ontology. In this way, an a-priori knowledge base is formed and used as a basis for its further exploitation within semantic image analysis and reasoning support.

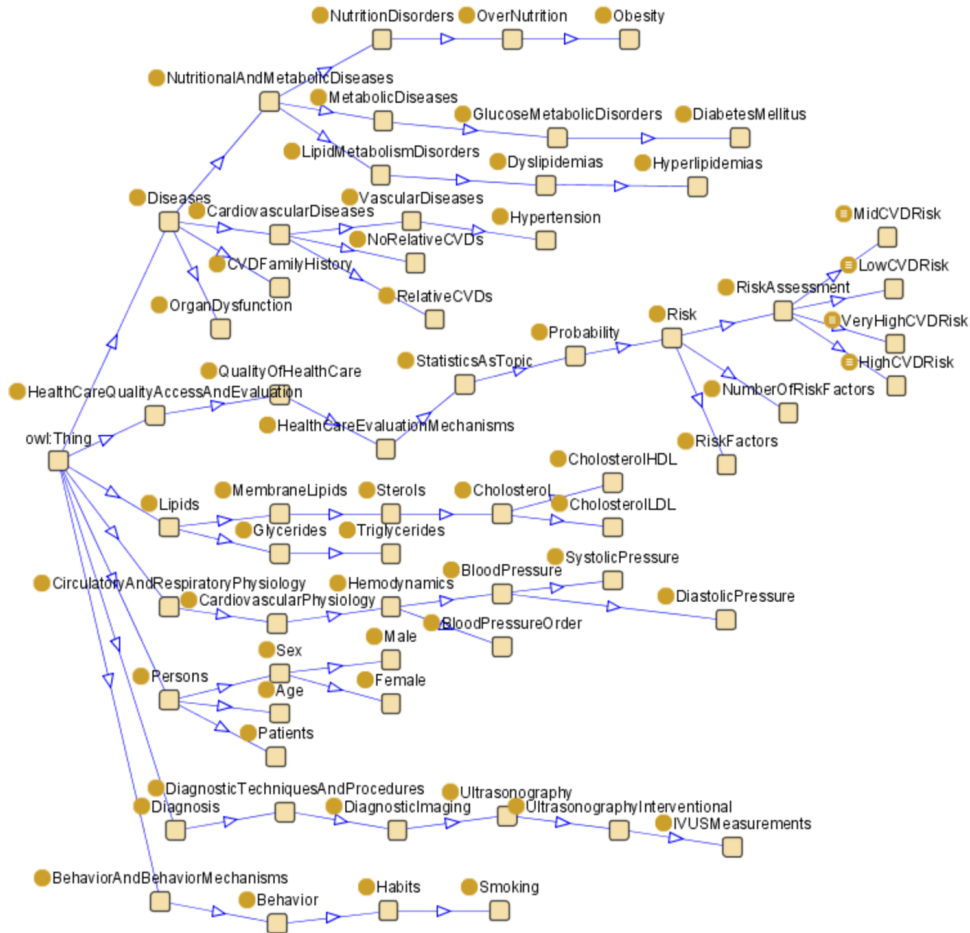
Figure 6 Semantic patient classification (see online version for colours)



3.1 Ontology description

The domain ontology in the semantic analysis system implementation (Figure 7) was based on the MeSH thesaurus as explained earlier in this section. Given the guidelines provided by the medical experts, in addition to the risk factors that would be taken into account for the overall patient classification scheme, the appropriate concepts from the thesaurus were selected to form the ontology where the system would be based on. As a result, the scalability of this approach is enhanced due to the reasons discussed earlier.

Figure 7 The domain ontology (see online version for colours)



Additional classes had to be added to the ontology for domain-specific concepts as was done with e.g., Low, Mid, High and Very High CVD Risk, which were added as subclasses to the Risk Assessment class (MeSH ID: D018570). Given that the ontology would serve both as patient data repository as well as knowledge base, where new knowledge would be generated, overall development was tested so as to ensure adequate data representation, retrieval and storage coupled with the ability to efficiently perform reasoning.

More specifically, the repository for which the ontology will be the bone structure should be able to effectively store and retrieve patient information for the purpose of data viewing, but it should also be made easy to handle when it comes to performing reasoning either rule- or DL-based. Keeping these in mind, the ontology has five main classes, which are in turn broken down to subclasses representing the specific concepts we are trying to describe. These classes are:

- *Diseases*: Is divided in concepts regarding the description of diseases. These can be metabolic diseases like *Diabetes*, CVDs like *Hypertension* and so on
- *Health care quality access and evaluation*: Concepts like *Medical Record*, *Risk Assessment* and *Risk Factors* are subclasses of this class.
- *Lipids*: *Cholesterol* and *Triglycerides* values from biochemical tests are stored here.
- *Diagnosis*: IVUS morphometric measurements, calculated using the methodology described in Section 2, are stored in this class hierarchy. The class *IVUS Measurement* was not part of the MeSH thesaurus so it was added accordingly under *Ultrasonography Interventional* for the purposes of this work.
- *Risk assessment*: Under this class are the classes Low, Mid, High and Very High CVD Risk, which correspond to the patient risk category classes. These classes were not part of the MeSH thesaurus so they were added accordingly.

To sum up, data from three different sources (Medical Record information, Biochemical tests results and IVUS morphometric measurements) are integrated in the ontology. Medical Record information includes Age, Sex and if the patient suffers from Hypertension, Hyperlipidemia, Diabetes or Obesity. Additional info for Smoking and CVD family history are referred here. Biochemical test results correspond to Cholesterol levels, values of Triglycerides and LDL/HDL cholesterol. Finally, IVUS measurements include Maximum Wall Thickness (maxWT) of the artery and the ratio of Minimum Wall Thickness to Maximum Wall Thickness, known as Eccentricity Index (EI).

3.2 Reasoning and semantic rules

As mentioned earlier, the semantic analysis system consists of a medical ontology representing the medical concepts related to the CVD, by means of classes and class hierarchy. Moreover, it takes advantage of the powerful functionalities of the Semantic Web, by applying SWRL rules on top of the ontology to perform reasoning about the risk factors of each individual patient and predict the corresponding risk assessment of the disease. The implementation of both the ontology and the semantic reasoning is based on the KAON2 reasoner (Motik and Sattler, 2006).

The application of DL reasoning and semantic rules, on top of the domain ontology, simulates and expresses in an algorithmic form the process that experts follow to deduce facts, extract new knowledge and render the implicit knowledge explicit (Hussain et al., 2007; Ruffolo et al., 2007). It is relatively straightforward to map structured or semi-structured data ontology instances.

Eventually, the new extracted knowledge is stored back in the knowledge base, expanding it in every single step of the process (Figure 6). In conclusion, our approach offers the possibility of data integration from multiple heterogeneous sources, analysis and enhancement of the existing knowledge base with new facts concerning the medical data given as input.

In most reasoning systems that use ontologies, the demanded knowledge to enable reasoning support (e.g., the factors that affect the disease behaviour and development rates) is embodied in the application code or in custom rules used in combination with the domain ontology. It is important to mention that precise and consistent characterisation of the relation terms leads to more precise definition and description of the information represented in the ontology and, as a result, to stronger and more effective automated reasoning. In addition, the problem of combining rules with ontology languages has attracted a lot of attention, and recent research efforts have yielded the proposal of rule languages specific to the Semantic Web (RuleML, SWRL). Kashyap et al. (2006) used a business rule engine in combination with an OWL ontology to model clinical guidelines, with the latter being used mainly as a means to minimise the rule base rather than semantically describe their application domain.

3.2.1 *Syntax and semantics*

SWRL (Horrocks et al., 2004) is an acronym for Semantic Web Rule Language. SWRL is based on a combination of the OWL DL and OWL Lite sublanguages with the Unary/Binary RuleML Datalogue sublanguages of the Rule Markup Language and expressed through both an XML and an RDF concrete syntax. The basic idea of SWRL is to extend OWL DL, while maintaining the maximum backwards compatibility with OWL's existing syntax and semantics. Therefore, all rules are expressed in terms of OWL concepts (classes, properties, individuals, literals, etc.). SWRL includes a high-level abstract syntax for Horn-like rules in both the OWL DL and OWL Lite sublanguages (Dean et al., 2003) and provides powerful reasoning and calculation capabilities. SWRL rules go beyond basic Horn clauses in allowing conjunctive consequents, class descriptions as well as class predicates as predicates in class atoms and mathematical functions and therefore extremely expressive for the representation of typical medical guidelines.

3.2.2 *SWRL rules for CVD risk prediction*

In the current implementation of the risk prediction system, SWRL rules are used on top of the domain ontology to perform semantic reasoning concerning the health condition of the individuals-patients. As a first step, SWRL rules are used for reasoning in three different directions. More specifically, they reason about the concepts of the *Patient* class, the *Biochemical Data* class and the *IVUS Data* class, assigning the corresponding number of risk factors for each patient. Figure 8(b) demonstrates all the key risk factors for the evolvement of the disease taken into account in the proposed model. The second step deals with the application of the medical guidelines followed by the physicians, represented in Figure 8(a). This categorisation was selected after careful and elaborate study of the medical information and the official medical procedures performed during the evaluation of the risk degree. We continue with examples, in a human-readable format, demonstrating the 'algorithmic' flow of both levels of the applied SWRL rules. However, not all factors involved in each step of the reasoning procedure are demonstrated due to simplicity reasons.

For instance, consider the rule where age is considered as a risk factor. If a male patient's age is more than 45 years, then an appropriate rule should assign the age risk factor. The same rule should also consider the patient's sex as for female patients the age threshold is set to 55 years. The rule, expressed in a simplified form, which will handle this clinical guideline, is:

```

IF (hasGender(patient) == Male) THEN
  IF (hasAge(patient) > 45) THEN
    AssignAgeRiskFactor(patient)
ELSE
  IF (hasAge(patient) > 55) THEN
    AssignAgeRiskFactor(patient)

```

A similar rule that would express the guideline of EI, an important parameter that is calculated from the IVUS morphometric measurements and is defined as $EI = (\max WT - \min WT) / \max WT$, is formulated as:

```

IF (hasEI(patient) > 0.3) THEN
  AssignEIRiskFactor(patient)

```

After the determination of risk factors for each of the patients, the second level of classification would be to assign each patient to a risk category according to the guidelines depicted in Figure 10(a). Inspection of these guidelines reveals that risk categorisation involves not only the number of risk factors, but other parameters like arterial pressure or the presence of diabetes, thus making the classification more complex. For evaluation purposes, two methods for patient categorisation were introduced. The first one categorises patients using OWL definitions and restrictions, while the second uses SWRL rules as previously described for risk factor determination. As an example, the Mid-CVD Risk guideline will be used. Expressing the table from Figure 10(a) in natural language yields:

*A patient is in medium risk for developing a CVD IF he/she suffers from one or two risk factors **and** has arterial pressure of 1st **or** 2nd degree **OR** he/she suffers from no risk factors **and** has arterial pressure of 2nd degree.*

The guideline can be logically divided into two parts separated by the **OR**. Translation in OWL definitions yields:

$$\text{MidCVDRisk} \equiv (((\exists \text{hasArterialPressureDegree } (\text{Degree}_1 \cup \text{Degree}_2)) \cap (\exists \text{hasNumberOfRiskFactors } \text{OneOrTwoRFs})) \cup ((\exists \text{hasArterialPressureDegree } \text{Degree}_2) \cap (\exists \text{hasNumberOfRiskFactors } \text{ZeroRFs})))$$

The same guideline translated in SWRL would need to be broken down to two logical parts it consists of. In human-readable SWRL form, it will be expressed as:

```

isInRiskCategory(?patient, MidCVDRisk) ← hasArterialPressureDegree(?patient,
(Degree_1 ∨ Degree_2)) ∧ hasNumberOfRiskFactors(?patient, OneOrTwoRFs)
isInRiskCategory(?patient, MidCVDRisk) ← hasArterialPressureDegree(?patient,
Degree_1) ∧ hasNumberOfRiskFactors(?patient, ZeroRFs)

```

From the above rule and OWL definitions, it can be observed that their formulation follows the natural language expression of the guidelines of Figure 10. Using the above methodology, all the guidelines of Figure 10(b) were translated in SWRL rules, while the

risk classification of Figure 10(a) was formulated in both SWRL rules and OWL definitions for the purposes of the evaluation discussed in Section 4.

Figure 8 (a) Guidelines used for patient risk classification and (b) patient risk factors incorporated in the knowledge base (see online version for colours)

	1 st degree SAP 140-159 or DAP 90-99	2 nd degree SAP 160-179 or DAP 100-109	3 rd degree SAP \geq 180 or DAP \geq 110
I – no Risk Factors	Low Risk	Mid Risk	High Risk
II – 1 or 2 Risk Factors	Mid Risk	Mid Risk	Very High Risk
III - \geq 3 Risk Factors or Organ Damage or Diabetes	High Risk	High Risk	Very High Risk
IV – Other Relative CVDs	Very High Risk	Very High Risk	Very High Risk

SAP = Systolic Artery Pressure, DAP = Diastolic Artery Pressure, WHO guidelines

(a)

Biochemical Data	
Cholesterol	>200
LDL	>160
HDL	<40
Triglycerides	>200
IVUS Data	
Maximum Wall Thickness (MaxWT)	>0.5mm
EI	>0.3
(Minimum Wall Thickness / Maximum Wall Thickness)	<0.3
Patient Data	
Hypertension	Hyperlipidemia
Diabetes	Smoking
CVD family history	Obesity
Sex	Male (Greater risk)
	Female (Lower risk)
Age	>45 for men
	>55 for women

(b)

4 Evaluation and discussion

4.1 IVUS segmentation method evaluation

The developed IVUS image analysis methodology of Section 2 was applied to a set of 40 images randomly selected from a pool of approximately 300 images belonging to five

different human arterial segments; 40 randomly selected images were segmented manually by experts to generate ground truth results. The arterial segments were captured using a mechanical imaging system and a 2.6 F sheath-based catheter, incorporating a 40 MHz single-element transducer rotating at 1800 rpm and generating 30 images/s. A motorised pullback device was used to draw out the catheter at a constant speed of 0.5 mm/s. The ultrasound data were recorded in a 0.5-inch S-VHS videotape. The S-VHS data were digitised by a frame grabber integrated to the IVUS console at 512×512 pixels with 8-bit grey scale in a rate of 7.5 images/sec and the end-diastolic images were selected (peak of *R*-wave on ECG). Indicative results of the proposed approach on the employed data set are presented in Figure 9, where the boundaries manually detected by a domain expert are also shown, along with results from our previous approach.

Figure 9 Indicative experimental results of the proposed approach (b), (d), (f), (h), (j) and corresponding contours manually generated by experts (a), (c), (e), (g), (i)

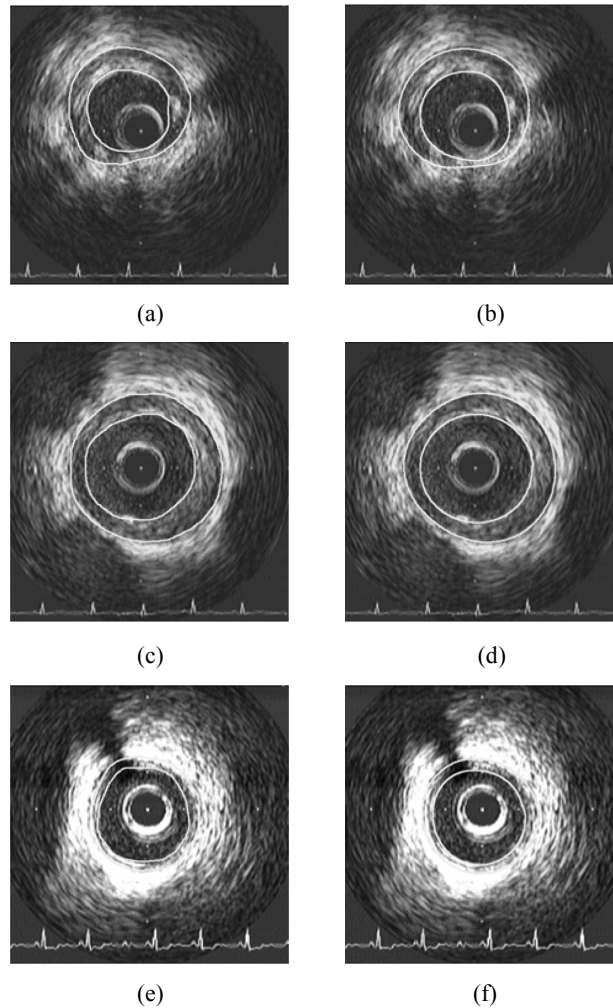
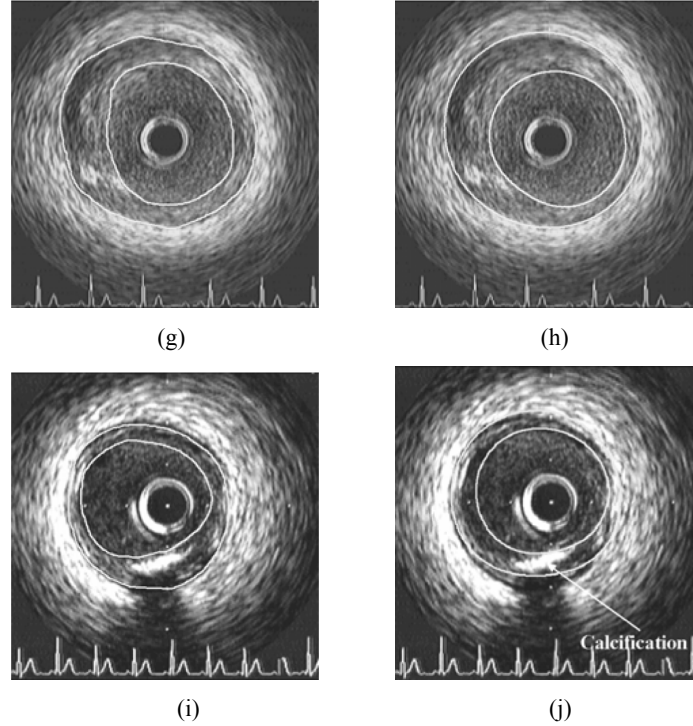


Figure 9 Indicative experimental results of the proposed approach (b), (d), (f), (h), (j) and corresponding contours manually generated by experts (a), (c), (e), (g), (i) (continued)



The results seem consistent with the ground truth data generated by experts, showing good contour localisation. These results are further exploited in this work by providing the basis for the estimation of various morphometric measures of the vessel as is the maximum and minimum wall thickness or the lumen radius. Additionally, these contours can be used for the 3D reconstruction of the vessel model. Table 2 summarises the mean differences between manually and automatically generated results ($Md \pm SD$, i.e., mean and standard deviation of the differences between automated and manual tracings) for three IVUS parameters, namely lumen, vessel and wall area. The results reveal that the proposed method performs adequately well, showing small differences from the ground truth measurements. Papadogiorgaki et al. (2008) provide comparison results of other methods for automatic IVUS segmentation to the proposed approach, which prove its superiority.

Table 2 Mean difference and standard deviation between automated and manually generated results regarding three IVUS parameters. LCSA = Lumen Cross Section Area, VCSA = Vessel Cross Section Area, WCSA = Wall Cross Section Area

<i>Lumen area (LCSA, mm²)</i>	<i>Vessel area (VCSA, mm²)</i>	<i>Wall area (WCSA, mm²)</i>
0.127 ± 1.209	0.059 ± 1.589	-0.067 ± 1.363

4.2 Semantic analysis evaluation

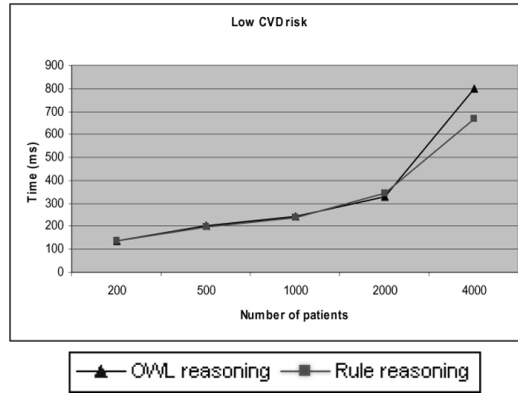
Using the methodology and system architecture described in Section 3, we were able to evaluate the risk factors and assess the danger for patients developing CVDs. We were able to test the system to measure its scalability in terms of knowledge base size and draw conclusions based on these measures. Another interesting part of the employed evaluation was the performance difference measurement for query answering between pure rule-based reasoning for decision-making and the combined use of rule-based and OWL reasoning.

For this purpose, two configurations of the knowledge base were used. In the first, SWRL rules were used for the determination of the risk factors each patient had, a process that includes numerical comparisons and mathematical calculations, and final judgement on risk categorisation was decided using OWL reasoning by appropriate formulation of conditions in each of the *Low*, *Mid*, *High* and *Very High CVD Risk* classes. In the second configuration, pure SWRL rule-based reasoning was used for both risk factor determination and risk categorisation. For each configuration, the mean response time for a set of queries was measured when the knowledge base was populated with a different number of patients (instances). Figure 10 shows the results for four queries to the knowledge base asking to retrieve the patients who belong to each of the Risk Category classes. Note that the choice between using rule- and OWL-based reasoning is not always feasible, as some reasoning tasks can be too complex to be formulated into OWL restrictions only, as is the case e.g., with numerical comparisons, so rules have to be used for that purpose.

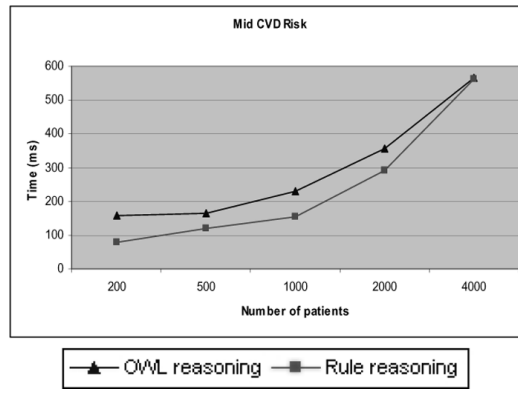
Some interesting conclusions can be drawn from these tests. It can be seen that the rise in response time is not always proportional to the number of patients (instances) that are integrated in the knowledge base. For example, regarding the rule-reasoning case, in Figure 10(d), doubling the number of patients from 500 to 1000 brings an increase in response time from 91 ms to 120 ms (32% increase) while increasing from 1000 to 2000 patients response time is almost tripled as it rises from 120 ms to 343 ms (185% increase). The same stands for Figure 10(c) where increasing from 2000 to 4000 patients increases response time from 266 to 739 (178% increase). Differences in performance are not as significant when OWL-based reasoning is applied. However, what can be seen in both cases is that there seems to be a critical point after which an increase in instances number has an unproportionally large increase in response time and it is different for every rule or OWL class definition as it depends on their complexity. For example, in Figure 10(c) for rule-based reasoning, this point mark is at 2000 patients, while for OWL-based it is at 1000. It should be noted that adding one patient to the ontology adds not only one but many more instances in the knowledge base, typically one for every property of the patient. This performance variability seems to originate from the KAON2 reasoner that was used and how it is optimised to handle large numbers of instances. More information on KAON2 performance details can be found in Hustadt et al. (2007).

Additionally, a direct observation of the above charts reveals that the performance in terms of response time for rule-based and OWL-based reasoning is almost similar with a small favour over rule-based reasoning. This is true for almost every case except from Figure 10(c) and 10(d) at the 4000 and 2000 patients mark, respectively, where OWL reasoning has a slightly better response time. This variation in performance derives from rule and OWL definitions formulation.

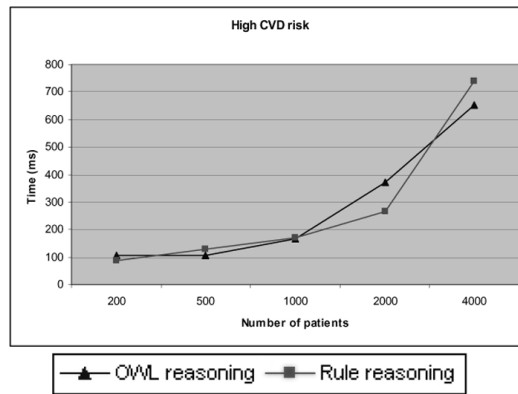
Figure 10 Response time of the system regarding querying for patients in each of the risk categories using pure rule based reasoning and mixed OWL + rule based reasoning: (a) low CVD risk; (b) mid CVD risk; (c) high CVD risk and (d) very high CVD risk



(a)

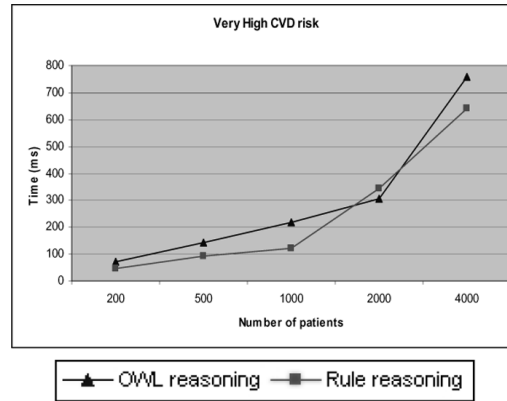


(b)



(c)

Figure 10 Response time of the system regarding querying for patients in each of the risk categories using pure rule based reasoning and mixed OWL + rule based reasoning: (a) low CVD risk; (b) mid CVD risk; (c) high CVD risk and (d) very high CVD risk (continued)



(d)

According to the above observations, it is shown that when there is a choice between using rule- or OWL-based reasoning, in terms of actual system performance, it makes a small difference on which to choose. The largest response time difference in absolute numbers was 132 ms (Figure 10(a) for 4000 patients), which corresponds to a 16% difference. Which type of reasoning shall be used is clearly a matter of knowledge base design principles and convenience. Using rule-based reasoning, developers and rule authors can make changes or corrections to the reasoning process more easily as rules can be edited, added or removed with ease, while with OWL-based reasoning there is a more concrete integration of domain knowledge and restrictions within the ontology and the knowledge base.

5 Conclusions and future work

We have presented a system that has the capability of performing risk assessment for CVDs by integrating patient data from different modalities. A method for the automatic detection of lumen borders in IVUS images, which makes use of texture characteristics and employing RBF approximation, was presented. Results of this method are illustrated and are very promising by showing great similarity to the actual ground truth images.

Measurements regarding the arterial wall thickness and lumen diameter are automatically extracted from IVUS images and are combined along with biochemical and medical record patient data to populate a knowledge base constructed specifically for CVD risk prediction. The ontology of the knowledge base is authored in OWL and reasoning is performed using rules expressed in SWRL and OWL reasoning. This proposed approach was evaluated, in terms of performance, against a system developed to use pure rule-based reasoning where it was shown that there is no actual difference between OWL- and rule-based reasoning. The evaluation concluded that the type of

reasoning to be employed should be decided having design principles in mind, rather than performance enhancement.

The proposed architecture could be the basis for integration of a larger set of medical methodologies in clinical care as guidelines specify the practices that are intended to provide safety and quality in patient care. The ontology of the proposed system was authored based on standard definitions of the medical field and it can be easily extended to support a wider range of clinical cases. As is shown, guidelines could be either added as rules or as OWL definitions depending on development choice.

Future work that will deal with the implementation of a graphical user interface for the insertion of patient's data, and for easy viewing of the results is currently being developed in close cooperation with the medical staff on the project. Additionally, the system has to be tested in a hospital environment to be able to evaluate its clinical usefulness and applicability in real-life cases, as is the case with the development of every medical system.

Acknowledgements

The work presented in this paper is supported by the A8-PPK06 project "Development of Techniques for the Semantic Processing of 3D Intravascular Ultrasound" funded by 50% from the European Union and by 50% from GSRT, Greece.

References

- Bom, M., Li, W., van der Steen, A.F., Lancee, C.T., Cespedes, E.I., Slager, C.J. and de Korte, C.L. (1998) 'New developments in intravascular ultrasound imaging', *Eur. J. Ultrasounds*, Vol. 7, No. 1, pp.9–14.
- Brusseau, E., de Korte, C., Mastik, F., Schaar, J. and van der Steen, A. (2004) 'Fully automatic luminal contour segmentation in intracoronary ultrasound imaging – a statistical approach', *IEEE Trans. Med. Imag.*, Vol. 23, pp.554–566.
- Cardinal, M.H.R., Meunier, J., Soulez, G., Maurice, R., Therasse, E. and Cloutier, G. (2006) 'Intravascular ultrasound image segmentation: a three-dimensional fast-marching method based on gray level distributions', *IEEE Trans. Med. Imag.*, Vol. 25, No. 5, pp.590–601.
- Carr, J., Beatson, R., Cherrie, J., Mitchell, T., Fright, W., McCallum, B. and Evans, T. (2001) 'Reconstruction and representation of 3D objects with radial basis functions', *Proc. 28th Annual Conference on Computer Graphics and Interactive Techniques*, Los Angeles, California, USA, pp.67–76.
- Dean, M., Connolly, D., Harmelen, F.V., Hendler, J., Horrocks, I., McGuinness, D.L., Patel-Schneider, P.F. and Stein, L.A. (2003) 'OWL web ontology overview: W3C Working Draft 12', *OWL Web Ontology Language*, <http://www.w3.org/TR/owl-ref>
- Filho, E.S., Yoshizawa, M., Tanaka, A., Saijo, Y. and Iwamoto, T. (2005) 'Detection of luminal contour using fuzzy clustering and mathematical morphology in intravascular ultrasound images', *Proc. 2005 IEEE Annual Conference on Engineering in Medicine and Biology (EMBS)*, Shanghai, China, pp.3471–3474.
- Giannoglou, G.D., Chatzizisis, Y.S., Sianos, G., Tsikaderis, D., Matakos, A., Koutkias, V., Diamantopoulos, P., Maglaveras, N., Parcharidis, G.E. and Louridas, G.E. (2006) 'In-vivo validation of spatially correct three-dimensional reconstruction of human coronary arteries by integrating intravascular ultrasound and biplane angiography', *Coron. Artery Dis.*, Vol. 17, No. 6, pp.533–543.

- Giannoglou, G.D., Chatzizisis, Y.S., Koutkias, V., Kompatsiaris, I., Papadogiorgaki, M., Mezaris, V., Parissi, E., Diamantopoulos, P., Strintzis, M.G., Maglaveras, N., Parcharidis, G.E. and Louridas, G.E. (2007) 'A novel active contour model for fully automated segmentation of intravascular ultrasound images: in vivo validation in human coronary arteries', *Computers Biol. Med.*, Vol. 37, pp.1292–1302.
- Glagov, S., Weisenberg, E., Zarins, C.K., Stankunavicius, R. and Kolettis, G.J. (1987) 'Compensatory enlargement of human atherosclerotic coronary arteries', *N. Engl. J. Med.*, Vol. 316, pp.1371–1375.
- Horrocks, I., Patel-Schneider, P.F., Boley, H., Tabet, S., Grosz, B. and Dean, M. (2004) *SWRL: A semantic Web Rule Language Combining OWL and RuleML*, <http://www.w3.org/Submission/SWRL>
- Hussain, S., Raza Abidi, S. and Raza Abidi, S.S. (2007) *Semantic Web Framework for Knowledge-Centric Clinical Decision Support Systems*, Lecture Notes in Computer Science, Vol. 4594, pp.451–455.
- Hustadt, U., Motik, B. and Sattler, U. (2007) 'Reasoning in description logics by a reduction to disjunctive datalog', *Journal of Automated Reasoning*, Vol. 39, No. 3, pp.351–384.
- Kashyap, V., Morales, A. and Hongsermeier, T. (2006) 'On implementing clinical decision support: achieving scalability and maintainability by combining business rules and ontologies', *AMIA 2006 Symposium Proceedings*, Washington, DC, USA, pp.414–418.
- Klingensmith, J., Nair, A., Kuban, B. and Vince, D. (2004) 'Segmentation of three-dimensional intravascular ultrasound images using spectral analysis and a dual active surface model', *IEEE Int. Ultrasonics Symposium*, Vol. 3, pp.1765–1768.
- Kovalski, G., Beyar, R., Shofti, R. and Azhari, H. (2000) 'Threedimensional automatic quantitative analysis of intravascular ultrasound image', *Ultrasound Med. Biol.*, Vol. 26, pp.527–537.
- Mario, C.D., Gorge, G., Peters, R., Kearney, P., Pinto, F., Hausmann, D., von Birgelen, C., Colombo, A., Mudra, H., Roelandt, J. and Erbel, R. (1998) 'Clinical application and image interpretation in intracoronary ultrasound', *Eur. Heart J.*, Vol. 19, pp.207–229.
- Mezaris, V., Kompatsiaris, I. and Strintzis, M. (2004) 'Still image segmentation tools for object-based multimedia applications', *Int. J. Pattern Recog. Artif. Int.*, Vol. 18, No. 4, pp.701–725.
- Motik, B. and Sattler, U. (2006) 'A comparison of reasoning techniques for querying large description logic ABoxes', *Proc. 13th International Conference on Logic for Programming Artificial Intelligence and Reasoning (LPAR 2006)*, Phnom Penh, Cambodia, pp.227–241.
- Nelson, S.J., Aronson, A., Doszkocs, T., Wilbur, J., Bodenreider, O., Chang, F., Mork, J. and McCray, A. (1999) 'Automated assignment of medical subject headings', *AMIA Annual Symposium*, Washington, DC, p.1127.
- Nelson, S.J., Powell, T. and Humphreys, B.L. (2002) 'The unified medical language system (UMLS) project', *Encyclopedia of Library and Information Science*, Marcel Dekker, Inc., New York, pp.369–378.
- Nissen, S.E. and Yock, P. (2001) 'Intravascular ultrasound: novel pathophysiological insights and current clinical applications', *Circulation*, Vol. 103, pp.604–616.
- Papadogiorgaki, M., Mezaris, V., Chatzizisis, Y.S., Giannoglou, G.D. and Kompatsiaris, I. (2007a) 'Texture analysis and radial basis function approximation for IVUS image segmentation', *The Open Biomedical Engineering Journal*, Vol. 1, pp.53–59.
- Papadogiorgaki, M., Mezaris, V., Chatzizisis, Y.S., Giannoglou, G.D. and Kompatsiaris, I. (2007b) 'Automated IVUS contour detection using intensity features and radial basis function approximation', *20th IEEE International Symposium on Computer-Based Medical Systems (CBMS 2007)*, Maribor, Slovenia, pp.183–188.
- Papadogiorgaki, M., Mezaris, V., Chatzizisis, Y.S., Giannoglou, G.D. and Kompatsiaris, I. (2008) 'Image analysis techniques for automated IVUS contour detection', *Ultrasound in Medicine and Biology*, Vol. 34, No. 9, pp.1482–1498.

- Plissiti, M., Fotiadis, D., Michalis, L. and Bozios, G. (2004) 'An automated method for lumen and media-adventitia border detection in a sequence of IVUS frames', *IEEE Trans. Inform. Tech. Biomed.*, Vol. 8, No. 2, pp.131–141.
- Rogers, J.E., Roberts, A., Solomon, W.D., van der Haring, E.J., Wroe, C.J., Zanstra, P.E. and Rector, A.L. (2001) 'GALEN ten years on: tasks and supporting tools', in Patel, V., Rogers, R. and Haux, R. (Eds.): *Proceedings of MEDINFO2001*, IOS Press, pp.256–260.
- Ruffolo, M., Manna, M., Cozza, V. and Ursino, R. (2007) 'Semantic clinical process management', *20th IEEE International Symposium on Computer-Based Medical Systems (CBMS'07)*, Jyväskylä, Finland, pp.518–523.
- Schoenhagen, P. and Nissen, S.E. (2002) 'Understanding coronary artery disease: tomographic imaging with intravascular ultrasound', *Heart*, Vol. 88, pp.91–96.
- Sonka, M., Zhang, X., Siebes, M., Bissing, M., DeJong, S., Collins, S. and McKay, C. (1995) 'Segmentation of intravascular ultrasound images: a knowledge-based approach', *IEEE Trans. Med. Imag.*, Vol. 14, pp.719–732.
- Unal, G., Bucher, S., Carlier, S., Slabaugh, G., Fang, T. and Tanaka, K. (2006) 'Shape-driven segmentation of intravascular ultrasound images', *Proc. 1st International Workshop on Computer Vision for Intravascular and Intracardiac Imaging (CVII 2006) at MICCAI 2006*, Copenhagen, Denmark, October, pp.51–58.
- Unser, M. (1995) 'Texture classification and segmentation using wavelet frames', *IEEE Trans. Image Process.*, Vol. 4, No. 11, pp.1549–1560.

Websites

American Heart Association, <http://www.americanheart.org>

FarField Technology, <http://www.farfieldtechnology.com>

KAON2: Ontology Management for the Semantic Web, <http://kaon2.semanticweb.org>

MeSH thesaurus, <http://www.nlm.nih.gov/mesh>

The OpenGALEN Ontology of Human Anatomy, <http://www.opengalen.org/open/crm/crm-anatomy.html>

UMLS, <http://www.nlm.nih.gov/research/umls>